Mathematics Interdisciplinary Research **11** (2) (2026) 141 − 159

Original Scientific Paper

A High-Performance Block-Based Computational Scheme for Solving Fractional Nonlinear Equations in Electrospinning Modeling

Hadis Azin and *Yadollah Ordokhani*⋆

Abstract

The Bratu-type equation of fractional order possesses considerable theoretical and applied importance, as it generalizes a conventional nonlinear differential equation to model phenomena that exhibit inherent memory and non-local interactions, which are crucial in fields such as nuclear reactor assessment and the electrospinning process of nanofibers. This study presents an innovative block-by-block (multi-step) computational methodology that employs quadratic interpolation to attain high-order accuracy. The approach ensures a convergence rate of order $\mathcal{O}(\tau^4)$, significantly enhancing numerical precision concerning the discretization parameter τ. Its practical utilization is illustrated through a dedicated algorithm tailored for the fractional Bratu problem. The effectiveness and robustness of the proposed method are validated through numerical experiments, showcasing its ability to deliver high-fidelity solutions.

Keywords: Block-by-block scheme, Quadratic interpolation, Fractional Bratu equation, Caputo derivative.

2020 Mathematics Subject Classification: 34A08; 65L20; 41A55.

How to cite this article
H. Azin and Y. Ordokhani, A high-performance block-based computational scheme for solving fractional nonlinear equations in electrospinning modeling, *Math. Interdisc. Res.* **11** (2) (2026) 141-159.

⋆Corresponding author (E-mail: ordokhani@alzahra.ac.ir)
Academic Editor: Akbar Mohebbi
Received 25 September 2025, Accepted 3 February 2026
DOI: 10.22052/MIR.2026.257657.1542

1. Introduction

The development of fractional differential equations, with historical roots in the 17th century, marks a significant evolution from classical calculus by enabling the modeling of systems with inherent memory and non-local interactions. While initially a mathematical abstraction, fractional differential equations have transcended into a critical paradigm across diverse fields, including viscoelasticity, control systems, biological transport phenomena, and financial modeling, due to their unique capacity to encapsulate complex hereditary dynamics and long-range dependencies more accurately than integer-order counterparts [1–6]. Consequently, the transition of fractional differential equations from theoretical curiosity to practical necessity underscores their indispensable role in advancing the mathematical description of real-world complexity.

The classical Bratu equation, a seminal nonlinear eigenvalue problem, is renowned for modeling thermal combustion and serves as a fundamental benchmark for numerical solvers [7]. Its fractional counterpart generalizes this framework by incorporating non-local operators, enabling the modeling of anomalous diffusion and memory-dependent phenomena in complex systems. This evolution from integer-order to fractional-order formulation exemplifies the broader paradigm shift in applied mathematics toward fractional calculus.

The fractional Bratu differential equation, employing the Caputo fractional derivative operator, is expressed as a nonlocal nonlinear initial value problem governed by

$$ {}_0^cD_t^\gamma y(t) + \xi_0 e^{\xi_1 y(t)} = 0, \qquad 0 \le t \le T, \quad 1 < \gamma \le 2, \tag{1} $$

with $y(0) = a_0$ and $y'(0) = a_1$. In general, the existence and uniqueness of solutions to equations of the form ${}_0^cD_t^\gamma y(t) = \mathscr{F}\big(t, y(t)\big)$ are contingent upon the fulfillment of a Lipschitz condition by the nonlinear term $\mathscr{F}$ (see[8]).

Due to the inherent non-locality and hereditary properties introduced by fractional order operators, analytical solutions to such equations are seldom attainable, necessitating the formulation and application of specialized numerical methods tailored for fractional differential equations. The approach presented in [9] utilizes an operational matrix technique founded on fractional-order Lagrange orthogonal polynomials, which transforms the governing fractional Bratu equation into a system of algebraic equations via spectral projection. In [10], a neural network framework incorporating rational activation functions is introduced to derive numerical approximations for Bratu-type equations through machine learning-based optimization techniques. Latif et al. introduced a collocation scheme employing spline functions, wherein piecewise polynomial approximations are formulated on discretized domains to obtain numerical solutions to the nonlinear Bratu problem [11]. Also, researchers developed a hybrid Chebyshev-block-pulse wavelets method to solve the fractional Bratu equation, transforming it into an algebraic system. The method's convergence was established, and numerical results confirmed its accuracy across various fractional orders and parameters [12]. The Adomian de-

composition transform method was developed by combining the Jafari transform with Adomian decomposition to solve fractional Bratu-type equations [13]. Taylor expansions were employed to accelerate convergence of nonlinear terms. A generalized form of the higher-order nonlinear fractional Bratu-type equation was introduced, utilizing a generalized fractional derivative for broader applicability and the homotopy perturbation transform method was employed to solve [14]. For comprehensive methodological details and further numerical analyses, readers are referred to the relevant literature [15–24].

The advancement of these refined computational methodologies marks substantial progress in addressing nonlinear fractional-order problems, providing powerful analytical tools for research applications in applied mathematics and engineering disciplines. This research introduces a high-precision computational technique that integrates quadratic Lagrange interpolation within a block-by-block framework for solving the nonlinear fractional model specified in Equation (1), attaining fourth-order convergence. The original formulation is first converted into an equivalent Volterra integral equation, which is subsequently discretized to yield a system of algebraic equations. The solution domain is subdivided into $2m$ uniform segments, facilitating local approximations of $y(t)$ using quadratic polynomials at nodal points.

The structure of this paper is organized as follows: Section 2 provides the necessary foundational concepts of fractional calculus. The computational algorithm and its numerical implementation are elaborated in Section 3. A rigorous convergence analysis is established in Section 4. Extensive numerical experiments demonstrating the efficacy of the proposed scheme are presented in Section 5. Finally, Section 6 concludes the study by summarizing the principal findings and discussing their broader implications for the field of computational mathematics.

2. Fractional calculus preliminaries

This section establishes the mathematical foundations necessary for the formal characterization of essential fractional calculus operators and their principal properties.

Definition 2.1. ([25]). The Riemann-Liouville fractional integral of order γ, where $\gamma > 0$, for a function $F(t)$ defined on the interval $[z_1, z_2]$, is formally represented by

$$ {}^{RL}_{z_1}I^{\gamma}_{t}F(t) = \frac{1}{\Gamma(\gamma)} \int_{z_1}^{t} (t-v)^{\gamma-1} F(v)dv. \tag{2}$$

Definition 2.2. ([25]). The Caputo fractional derivative (left-sided) of order γ with $r-1 < \gamma \leq r \in \mathbb{N}$, for a sufficiently smooth function $F(t)$ on the interval

$t \in [z_1, z_2]$ is defined as follow:

$$ {}_{z_1}^{c}D_t^{\gamma} F(t) = \begin{cases} \dfrac{1}{\Gamma(r-\gamma)} \displaystyle\int_{z_1}^{t} (t-v)^{r-\gamma-1} F^{(r)}(v)dv, & r-1 < \gamma < r, \\ F^{(r)}(t), & \gamma = r. \end{cases} \tag{3} $$

Lemma 2.3. *([25]). Assume $F(t)$ is sufficiently smooth on $[z_1, z_2]$. Then, relation between Riemann-Liouville fractional integral and the Caputo fractional derivative holds as:*

$$ {}_{z_1}^{RL}I_t^{\gamma} \left({}_{z_1}^{c}D_t^{\gamma} F(t) \right) = F(t) - \sum_{k=0}^{r-1} \frac{F^{(k)}(z_1)}{\Gamma(k+1)} (t-z_1)^k, \qquad r-1 < \gamma \leq r. \tag{4} $$

3. Formulation of the multi-step approach

This section develops a high-accuracy computational scheme for addressing the fractional initial value problem given in Equation (1). The adopted approach commences with the conversion of the original differential problem into an equivalent Volterra-type integral equation by applying Riemann-Liouville integration to both sides and Lemma 2.3, resulting in the following expression:

$$ y(t) = a_0 + a_1 t - \frac{\xi_0}{\Gamma(\gamma)} \int_0^t (t-v)^{\gamma-1} e^{\xi_1 y(v)} dv. \tag{5} $$

A discretization of the computational domain $[0, T]$ is implemented by dividing it uniformly into $2m$ subintervals of equal length $\tau = \frac{T}{2m}$, with nodes specified by $t_i = i\tau$ for $i = 0, 1, 2, \ldots, 2m$. Over each segment $[t_0, t_i]$, a quadratic interpolating polynomial $Y_i(t)$ is formulated to approximate $e^{\xi_1 y(t)}$, leading to the following

representation:

$$e^{\xi_1 y(t)} \simeq \begin{cases} Y_1(t) = \dfrac{2(t-t_{\frac{1}{2}})(t-t_1)}{\tau^2} e^{\xi_1 y_0} + \dfrac{-4(t-t_0)(t-t_1)}{\tau^2} e^{\xi_1 y_{\frac{1}{2}}} \\ \qquad + \dfrac{2(t-t_0)(t-t_{\frac{1}{2}})}{\tau^2} e^{\xi_1 y_1}, & [t_0, t_1], \\ Y_2(t) = \dfrac{(t-t_1)(t-t_2)}{2\tau^2} e^{\xi_1 y_0} + \dfrac{(t-t_0)(t-t_2)}{-\tau^2} e^{\xi_1 y_1} \\ \qquad + \dfrac{(t-t_0)(t-t_2)}{2\tau^2} e^{\xi_1 y_2}, & [t_0, t_2], \\ Y_{2i+1}(t) = Y_1(t) + \displaystyle\sum_{j=1}^{i} \dfrac{(t-t_{2j})(t-t_{2j+1})}{2\tau^2} e^{\xi_1 y_{2j-1}} \\ \qquad + \dfrac{(t-t_{2j-1})(t-t_{2j+1})}{-\tau^2} e^{\xi_1 y_{2j}} & [t_0, t_{2i+1}], \\ \qquad + \dfrac{(t-t_{2j})(t-t_{2j-1})}{2\tau^2} e^{\xi_1 y_{2j+1}}, \quad 1 \le i \le m-1, \\ Y_{2i+2}(t) = \displaystyle\sum_{j=0}^{i} \dfrac{(t-t_{2j+1})(t-t_{2j+2})}{2\tau^2} e^{\xi_1 y_{2j}} \\ \qquad + \dfrac{(t-t_{2j})(t-t_{2j+2})}{-\tau^2} e^{\xi_1 y_{2j+1}} & [t_0, t_{2i+2}], \\ \qquad + \dfrac{(t-t_{2j})(t-t_{2j+1})}{2\tau^2} e^{\xi_1 y_{2j+2}}, \quad 1 \le i \le m-1, \end{cases} \tag{6}$$

in which $t_{\frac{1}{2}} = t_0 + \frac{\tau}{2}$, $y_i = y(t_i)$ and the value $y_{\frac{1}{2}}$ is approximated through interpolation, yielding:

$$e^{\xi_1 y_{\frac{1}{2}}} \simeq \frac{3}{8} e^{\xi_1 y_0} + \frac{3}{4} e^{\xi_1 y_1} - \frac{1}{8} e^{\xi_1 y_2}. \tag{7}$$

Substituting the expressions from (7) into the corresponding relation (6) yields the approximation for $e^{\xi_1 y(t)}$ over the interval $[t_0, t_1]$ as:

$$\begin{aligned} Y_1(t) \simeq \Bigg(\frac{2(t-t_{\frac{1}{2}})(t-t_1)}{\tau^2} - \frac{3}{2} \frac{(t-t_0)(t-t_1)}{\tau^2} \Bigg) e^{\xi_1 y_0} + \Bigg(\frac{2(t-t_0)(t-t_{\frac{1}{2}})}{\tau^2} \\ - 3 \frac{(t-t_0)(t-t_1)}{\tau^2} \Bigg) e^{\xi_1 y_1} + \frac{1}{2} \frac{(t-t_0)(t-t_1)}{\tau^2} e^{\xi_1 y_{\frac{1}{2}}}. \end{aligned} \tag{8}$$

By incorporating the approximations (6) and (8) into (5), the numerical solution at each discretization point t_l for $l = 1, 2, \ldots, 2m$ can be expressed as:

$$y_1 \simeq a_0 + a_1 t_1 - \frac{\xi_0}{\Gamma(\gamma)} \int_0^{t_1} (t_1 - v)^{\gamma-1} Y_1(v) dv, \tag{9}$$

$$y_2 \simeq a_0 + a_1 t_2 - \frac{\xi_0}{\Gamma(\gamma)} \int_0^{t_2} (t_2 - v)^{\gamma-1} Y_2(v) dv, \tag{10}$$

$$y_{2i+1} \simeq a_0 + a_1 t_{2i+1} - \frac{\xi_0}{\Gamma(\gamma)} \int_0^{t_{2i+1}} (t_{2i+1} - v)^{\gamma-1} Y_{2i+1}(v) dv$$
$$= a_0 + a_1 t_{2i+1} - \frac{\xi_0}{\Gamma(\gamma)} \Bigg[\int_0^{t_1} (t_{2i+1} - v)^{\gamma-1} Y_1(v) dv + \sum_{j=1}^{i} \int_{t_{2j-1}}^{t_{2j+1}} (t_{2i+1} - v)^{\gamma-1}$$
$$\times \Bigg(\frac{(v - t_{2j})(v - t_{2j+1})}{2\tau^2} e^{\xi_1 y_{2j-1}} + \frac{(v - t_{2j-1})(v - t_{2j+1})}{-\tau^2} e^{\xi_1 y_{2j}}$$
$$+ \frac{(v - t_{2j})(v - t_{2j-1})}{2\tau^2} e^{\xi_1 y_{2j+1}} \Bigg) dv \Bigg], \tag{11}$$

and

$$y_{2i+2} \simeq a_0 + a_1 t_{2i+2} - \frac{\xi_0}{\Gamma(\gamma)} \int_0^{t_{2i+2}} (t_{2i+2} - s)^{\gamma-1} Y_{2i+2}(v) dv$$
$$= a_0 + a_1 t_{2i+2} - \frac{\xi_0}{\Gamma(\gamma)} \sum_{j=0}^{i} \int_{t_{2j}}^{t_{2j+2}} (t_{2i+2} - v)^{\gamma-1} \Bigg(\frac{(v - t_{2j+1})(v - t_{2j+2})}{2\tau^2} e^{\xi_1 y_{2j}}$$
$$+ \frac{(v - t_{2j})(v - t_{2j+2})}{-\tau^2} e^{\xi_1 y_{2j+1}} + \frac{(v - t_{2j})(v - t_{2j+1})}{2\tau^2} e^{\xi_1 y_{2j+2}} \Bigg) dv, \tag{12}$$

for $1 \leq i \leq m-1$. To simplify, it can be reformulated as:

$$y_1 \simeq a_0 + a_1 t_1 - \xi_0 \Big(\mathcal{G}_{1,0} e^{\xi_1 y_0} + \mathcal{G}_{1,1} e^{\xi_1 y_1} + \mathcal{G}_{1,2} e^{\xi_1 y_2} \Big), \tag{13}$$

$$y_2 \simeq a_0 + a_1 t_2 - \xi_0 \Big(\mathcal{G}_{2,0} e^{\xi_1 y_0} + \mathcal{G}_{2,1} e^{\xi_1 y_1} + \mathcal{G}_{2,2} e^{\xi_1 y_2} \Big), \tag{14}$$

$$y_{2i+1} \simeq a_0 + a_1 t_{2i+1} - \xi_0 \Big(\mathcal{G}_{1,0} e^{\xi_1 y_0} + \mathcal{G}_{1,1} e^{\xi_1 y_1} + \mathcal{G}_{1,2} e^{\xi_1 y_2}$$
$$+ \sum_{j=1}^{i} \mathcal{Z}_{1,2j-1} e^{\xi_1 y_{2j-1}} + \mathcal{Z}_{1,2j} e^{\xi_1 y_{2j}} + \mathcal{Z}_{1,2j+1} e^{\xi_1 y_{2j+1}} \Big), \tag{15}$$

and

$$y_{2i+2} \simeq a_0 + a_1 t_{2i+2} - \xi_0 \Big(\sum_{j=1}^{i} \mathcal{Z}_{2,2j} e^{\xi_1 y_{2j}} + \mathcal{Z}_{2,2j+1} e^{\xi_1 y_{2j+1}} + \mathcal{Z}_{2,2j+2} e^{\xi_1 y_{2j+2}} \Big), \tag{16}$$

in which

$$\mathcal{G}_{1,0} = \frac{1}{\tau^2 \Gamma(\gamma)} \int_0^{t_1} (t_1 - v)^{\gamma-1} \Big(2(v - t_{\frac{1}{2}})(v - t_1) - \frac{3}{2}(v - t_0)(v - t_1) \Big) dv, \tag{17}$$

$$\mathcal{G}_{1,1} = \frac{1}{\tau^2 \Gamma(\gamma)} \int_0^{t_1} (t_1 - v)^{\gamma-1} \Big(2(v - t_0)(v - t_{\frac{1}{2}}) - 3(v - t_0)(v - t_1) \Big) dv, \tag{18}$$

$$\mathcal{G}_{1,2} = \frac{1}{2\tau^2\Gamma(\gamma)} \int_0^{t_1} (t_1 - v)^{\gamma-1} \Big((v - t_0)(v - t_1) \Big) dv, \tag{19}$$

$$\mathcal{G}_{2,0} = \frac{1}{2\tau^2\Gamma(\gamma)} \int_0^{t_2} (t_2 - v)^{\gamma-1} \Big((v - t_1)(v - t_2) \Big) dv, \tag{20}$$

$$\mathcal{G}_{2,1} = \frac{-1}{\tau^2\Gamma(\gamma)} \int_0^{t_2} (t_2 - v)^{\gamma-1} \Big((v - t_0)(v - t_2) \Big) dv, \tag{21}$$

$$\mathcal{G}_{2,2} = \frac{1}{2\tau^2\Gamma(\gamma)} \int_0^{t_2} (t_2 - v)^{\gamma-1} \Big((v - t_0)(v - t_1) \Big) dv, \tag{22}$$

and

$$\mathcal{Z}_{1,2j-1} = \frac{1}{2\tau^2\Gamma(\gamma)} \int_{t_{2j-1}}^{t_{2j+1}} (t_{2i+1} - v)^{\gamma-1} \Big((v - t_{2j})(v - t_{2j+1}) \Big) dv, \tag{23}$$

$$\mathcal{Z}_{1,2j} = \frac{-1}{\tau^2\Gamma(\gamma)} \int_{t_{2j-1}}^{t_{2j+1}} (t_{2i+1} - v)^{\gamma-1} \Big((v - t_{2j-1})(v - t_{2j+1}) \Big) dv, \tag{24}$$

$$\mathcal{Z}_{1,2j+1} = \frac{1}{2\tau^2\Gamma(\gamma)} \int_{t_{2j-1}}^{t_{2j+1}} (t_{2i+1} - v)^{\gamma-1} \Big((v - t_{2j-1})(v - t_{2j}) \Big) dv, \tag{25}$$

$$\mathcal{Z}_{2,2j} = \frac{1}{2\tau^2\Gamma(\gamma)} \int_{t_{2j}}^{t_{2j+2}} (t_{2i+2} - v)^{\gamma-1} \Big((v - t_{2j+1})(v - t_{2j+2}) \Big) dv, \tag{26}$$

$$\mathcal{Z}_{2,2j+1} = \frac{-1}{\tau^2\Gamma(\gamma)} \int_{t_{2j}}^{t_{2j+2}} (t_{2i+2} - v)^{\gamma-1} \Big((v - t_{2j})(v - t_{2j+2}) \Big) dv, \tag{27}$$

$$\mathcal{Z}_{2,2j+2} = \frac{1}{2\tau^2\Gamma(\gamma)} \int_{t_{2j}}^{t_{2j+2}} (t_{2i+2} - v)^{\gamma-1} \Big((v - t_{2j})(v - t_{2j+1}) \Big) dv. \tag{28}$$

It is important to observe that every function is represented in relations of integrals (17) to (28) are polynomial. Consequently, can be computed exactly in explicit form for the specified parameters t_k and γ. The numerical procedure simplifies to solving the ensuing algebraic system in relations (13)-(16), which provides the discrete numerical approximation of the solution $y(t)$ at all nodal points.

4. Error analysis

This section is devoted to establishing the order of convergence for the fully discrete scheme formulated in the preceding section.

Theorem 4.1. *Assume $y(t) \in \mathcal{C}^3([0,T])$, and $\tilde{y}(t)$ denotes the numerical approximation of $y(t)$ at the nodal points with uniform step size τ. Moreover, every function $y^{(k)}(t)$ remains bounded over the entire domain $[0,T]$ for all $k = 0,1,2,3$. Indeed, we have*

$$\max_{0 \le t \le T} \left| y^{(k)}(t) \right| \le \mathcal{M}_k, \qquad k = 0,1,2,3. \tag{29}$$

Then, the convergence order of the proposed discrete scheme is $\mathcal{O}(\tau^4)$.

Proof. For the odd-indexed discretization points t_{2i+1}, $i = 0, 1, 2, \ldots, m-1$ the corresponding local truncation error using the relations (5), (6), (7) and (15) is expressed as:

$$\begin{aligned}
\left|y(t_{2i+1}) - \tilde{y}(t_{2i+1})\right| \leq \frac{\xi_0}{\Gamma(\gamma)} \int_0^{t_1} (t_{2i+1} - v)^{\gamma-1} \Bigg| \Bigg[e^{\xi_1 y(v)} \\
- \Bigg(\frac{2(v - t_{\frac{1}{2}})(v - t_1)}{\tau^2} e^{\xi_1 y_0} + \frac{-4(v - t_0)(v - t_1)}{\tau^2} e^{\xi_1 y_{\frac{1}{2}}} \\
+ \frac{2(v - t_0)(v - t_{\frac{1}{2}})}{\tau^2} e^{\xi_1 y_1} \Bigg) \Bigg] + \Bigg(e^{\xi_1 y(v_{\frac{1}{2}})} - \Big(\frac{3}{8} e^{\xi_1 y_0} + \frac{3}{4} e^{\xi_1 y_1} \\
- \frac{1}{8} e^{\xi_1 y_2} \Big) \Bigg) \frac{-4(v - t_0)(v - t_1)}{\tau^2} \Bigg| dv \\
+ \frac{\xi_0}{\Gamma(\gamma)} \sum_{j=1}^{i} \int_{t_{2j-1}}^{t_{2j+1}} (t_{2i+1} - v)^{\gamma-1} \Bigg| e^{\xi_1 y(v)} \\
- \frac{(v - t_{2j})(v - t_{2j+1})}{2\tau^2} e^{\xi_1 y_{2j-1}} + \frac{(v - t_{2j-1})(v - t_{2j+1})}{-\tau^2} e^{\xi_1 y_{2j}} \\
+ \frac{(v - t_{2j})(v - t_{2j-1})}{2\tau^2} e^{\xi_1 y_{2j+1}} \Bigg| dv.
\end{aligned} \tag{30}$$

By applying Taylor's theorem and the Lagrange remainder form, we obtain the following result for $\vartheta_1 \in [0, t_1]$, $\vartheta_2 \in [0, t_{\frac{1}{2}}]$ and $\vartheta_j \in [t_{2j-1}, t_{2j+1}]$ with $j = 1, 2, \ldots, i$ and $i = 1, 2, \ldots, m-1$:

$$\begin{aligned}
\left|\mathcal{R}_1(v)\right| = \Bigg| e^{\xi_1 y(v)} - \Bigg(\frac{2(v - t_{\frac{1}{2}})(v - t_1)}{\tau^2} e^{\xi_1 y_0} + \frac{-4(v - t_0)(v - t_1)}{\tau^2} e^{\xi_1 y_{\frac{1}{2}}} \\
+ \frac{2(v - t_0)(v - t_{\frac{1}{2}})}{\tau^2} e^{\xi_1 y_1} \Bigg) \Bigg| \leq \Bigg| \Big(y^{(3)}(\vartheta_1) + 3y''(\vartheta_1) y'(\vartheta_1) + \big(y'(\vartheta_1)\big)^3 \Big) e^{y(\vartheta_1)} \Bigg| \\
\times \frac{\left|(v - t_0)(v - t_{\frac{1}{2}})(v - t_1)\right|}{3!} \leq \frac{\big(\mathcal{M}_3 + 3\mathcal{M}_2\mathcal{M}_1 + \mathcal{M}_1^3\big) e^{\mathcal{M}_0} \tau^3}{3!},
\end{aligned} \tag{31}$$

$$\begin{aligned}
\left|\mathcal{R}_2(v)\right| = \Bigg| e^{\xi_1 y(v_{\frac{1}{2}})} - \Big(\frac{3}{8} e^{\xi_1 y_0} + \frac{3}{4} e^{\xi_1 y_1} - \frac{1}{8} e^{\xi_1 y_2} \Big) \Bigg| \leq \frac{\tau^3}{16} \Bigg| \Big(y^{(3)}(\vartheta_2) + 3y''(\vartheta_2) y'(\vartheta_2) \\
+ \big(y'(\vartheta_2)\big)^3 \Big) e^{y(\vartheta_2)} \Bigg| \leq \frac{\big(\mathcal{M}_3 + 3\mathcal{M}_2\mathcal{M}_1 + \mathcal{M}_1^3\big) e^{\mathcal{M}_0} \tau^3}{16},
\end{aligned} \tag{32}$$

and

$$\begin{aligned}\big|\mathcal{R}_j(v)\big| &= \Big|e^{\xi_1 y(v)} - \frac{(v-t_{2j})(v-t_{2j+1})}{2\tau^2}e^{\xi_1 y_{2j-1}} + \frac{(v-t_{2j-1})(v-t_{2j+1})}{-\tau^2}e^{\xi_1 y_{2j}} \\ &+ \frac{(v-t_{2j})(v-t_{2j-1})}{2\tau^2}e^{\xi_1 y_{2j+1}}\Big| \leq \Big|\Big(y^{(3)}(\vartheta_j) + 3y''(\vartheta_j)y'(\vartheta_j) + \big(y'(\vartheta_j)\big)^3\Big) \\ &\times e^{y(\vartheta_j)}\Big|\frac{\big|(v-t_{2j-1})(v-t_{2j})(v-t_{2j+1})\big|}{3!} \leq \frac{\big(\mathcal{M}_3 + 3\mathcal{M}_2\mathcal{M}_1 + \mathcal{M}_1^3\big)e^{\mathcal{M}_0}\tau^3}{3!}.\end{aligned} \tag{33}$$

This leads to the following key result:

$$\begin{aligned}\big|y(t_{2i+1}) - \tilde{y}(t_{2i+1})\big| &\leq \frac{\xi_0}{\Gamma(\gamma)}\int_0^{t_1}(t_{2i+1}-v)^{\gamma-1}\Big|\mathcal{R}_1(v) + \mathcal{R}_2(v)\frac{-4(v-t_0)(v-t_1)}{\tau^2}\Big|dv \\ &+ \frac{\xi_0}{\Gamma(\gamma)}\sum_{j=1}^{i}\int_{t_{2j-1}}^{t_{2j+1}}(t_{2i+1}-v)^{\gamma-1}\big|\mathcal{R}_j(v)\big|dv \\ &\leq \frac{\big(\mathcal{M}_3 + 3\mathcal{M}_2\mathcal{M}_1 + \mathcal{M}_1^3\big)e^{\mathcal{M}_0}\tau^3}{3!}\frac{\xi_0}{\Gamma(\gamma)}\int_0^{t_1}(t_{2i+1}-v)^{\gamma-1}dv \\ &+ \frac{4\big(\mathcal{M}_3 + 3\mathcal{M}_2\mathcal{M}_1 + \mathcal{M}_1^3\big)e^{\mathcal{M}_0}\tau}{16}\frac{\xi_0}{\Gamma(\gamma)}\int_0^{t_1}(t_{2i+1}-v)^{\gamma-1} \\ &\times \big|(v-t_0)(v-t_1)\big|dv \\ &+ \frac{\big(\mathcal{M}_3 + 3\mathcal{M}_2\mathcal{M}_1 + \mathcal{M}_1^3\big)e^{\mathcal{M}_0}\tau^3}{3!}\frac{\xi_0}{\Gamma(\gamma)}\sum_{j=1}^{i}\int_{t_{2j-1}}^{t_{2j+1}}(t_{2i+1}-v)^{\gamma-1}dv \\ &\leq \frac{\xi_0\big(\mathcal{M}_3 + 3\mathcal{M}_2\mathcal{M}_1 + \mathcal{M}_1^3\big)e^{\mathcal{M}_0}\tau^{3+\gamma}}{\Gamma(\gamma+1)}(2i+1)^{\gamma} - (2i)^{\gamma} \\ &+ \frac{\xi_0\big(\mathcal{M}_3 + 3\mathcal{M}_2\mathcal{M}_1 + \mathcal{M}_1^3\big)e^{\mathcal{M}_0}T^{\gamma}\tau^4}{\Gamma(\gamma+1)} \leq \mathscr{C}\tau^4,\end{aligned} \tag{34}$$

in which $\mathscr{C}$ is the positive constant. The truncation error at even-indexed steps can be evaluated in a manner identical to that demonstrated for the odd-indexed ones. The details are excluded here for the sake of conciseness, and this constructive process fully substantiates the theorem. □

5. Numerical results

This section employs the developed algorithm to examine the fractional nonlinear problem (1). Computational accuracy is assessed via the maximum norm, defined as:

$$\ell_\infty(\tau) = \max_{0\leq i\leq 2m}|y(t_i) - \tilde{y}(t_i)|, \tag{35}$$

in which $\tilde{y}(t_i)$ is an approximation of $y(t)$ at point t_i with time step τ. Moreover, the following relation is used to corroborate the theoretical convergence rates by

$$co = \frac{\log\left(\frac{\ell_\infty(\tau_1)}{\ell_\infty(\tau_2)}\right)}{\log\left(\frac{\tau_1}{\tau_2}\right)}. \tag{36}$$

Example 5.1. We examine the formulation of problem (1) given by

$$\begin{cases} {}_0^c D_t^\gamma y(t) - 2e^{y(t)} = 0, \quad 0 \le t \le 1, \\ y(0) = y'(0) = 0, \end{cases} \tag{37}$$

in which the analytical solution is $y(t) = -2\ln\big(\cos(t)\big)$ for $\gamma = 2$ [12, 22, 24]. The proposed computational framework was implemented to address the specified problem. Its performance was evaluated across a range of parameters γ and m. A comparative analysis of the absolute errors, presented in Table 1, confirms the accuracy of our method over the established techniques in [12, 24] for $\gamma = 2$. The experimental order of convergence, detailed in Table 2, aligns with the theoretical rate predicted by Theorem 4.1, thereby validating the algorithm's performance. A comparison between the exact and numerically obtained solutions for $m = 5$ is presented in Figure 1, considering several fractional orders $\gamma \in \{1.5, 1.6, 1.7, 1.8, 1.9\}$. The graphical results confirm the algorithm's efficiency and illustrate the convergence of the approximate solutions to the exact one as $\gamma \to 2$. A combined analysis of the quantitative data in Table 1, 2, and the graphical depictions in Figure 1 validates the effectiveness of our method. These results conclusively show that the numerical scheme is both successful and accurate for this category of nonlinear problems.

Example 5.2. In this numerical experiment, we examine the fractional equation (1), given by

$${}_0^c D_t^\gamma y(t) - e^{2y(t)} = 0, \tag{38}$$

on $t \in [0, 1]$ with the initial conditions $y(0) = y'(0) = 0$ and the true solution is $y(t) = \ln\big(\sec(t)\big)$ for $\gamma = 2$ [12, 22]. The developed numerical methodology was employed to solve the target problem, with its efficacy assessed over a comprehensive range of parameters γ and m. The empirical convergence rates and precision metrics, summarized in Table 3, corroborate the algorithm's high performance. In the absence of an analytical solution for the fractional-order cases, a direct computation of the absolute error is not feasible. To rigorously assess the accuracy and convergence of the proposed numerical scheme under these conditions, the problem is solved using two successive step sizes, τ_1 and τ_2. The difference between these numerical solutions at the common grid points provides a reliable measure of the scheme's stability and precision as follows:

$$\mathscr{E}_\infty = \big|y_{\tau_1}(T) - y_{\tau_2}(T)\big|, \tag{39}$$

Table 1: Comparison of the ℓ_∞ of the presented method with those obtained in [24] and [12] in Example 5.1.

t	[24]	[12]	Presented method
0	6.13×10^{-04}	6.22×10^{-29}	0
0.1	5.85×10^{-04}	4.78×10^{-06}	1.46×10^{-10}
0.2	6.19×10^{-04}	1.59×10^{-05}	2.61×10^{-10}
0.3	7.08×10^{-04}	2.99×10^{-05}	1.32×10^{-09}
0.4	8.03×10^{-04}	4.17×10^{-05}	1.05×10^{-09}
0.5	8.73×10^{-04}	4.57×10^{-05}	3.05×10^{-09}
0.6	9.42×10^{-04}	4.06×10^{-05}	2.43×10^{-09}
0.7	1.05×10^{-03}	2.81×10^{-05}	5.38×10^{-09}
0.8	1.21×10^{-03}	1.38×10^{-05}	4.44×10^{-09}
0.9	1.39×10^{-03}	2.67×10^{-06}	8.40×10^{-09}
1	1.72×10^{-03}	1.81×10^{-06}	7.21×10^{-09}
CUP Time (s)	–	–	3.250

in which $y_{\tau_1}(T)$ and $y_{\tau_2}(T)$ are the numerical solutions at the end of interval T with the step sizes τ_1 and τ_2, respectively. The results of this analysis are comprehensively presented in Table 4. A visual comparison of exact and approximate solutions for $m = 5$, displayed in Figure 2, encompasses multiple fractional orders γ. These results not only affirm the method's computational robustness but also demonstrate asymptotic convergence toward the exact solution as $\gamma \to 2$. Synthesizing insights from the quantitative assessments in Table 3 and the graphical representations in Figure 2, the proposed scheme validates the effectiveness as an accurate and reliable tool for this class of nonlinear fractional differential equations.

Example 5.3. Finally, the fractional main problem (1) is considered on the domain $t \in [0, 1]$ for $\xi_1 = 1$ with the following form:

$$ {}_0^c D_t^\gamma y(t) + \xi_0 e^{y(t)} = 0, \tag{40}$$

in which the exact solution is $y(t) = -2 \ln \left(\dfrac{\cosh\left((t - \frac{1}{2})\frac{\sigma}{2}\right)}{\cosh\left(\frac{\sigma}{2}\right)} \right)$ for $\gamma = 2$ and the value of σ is determined by solving the expression $\sigma = \sqrt{2\xi_0} \cosh\left(\frac{\sigma}{2}\right)$ [23]. The numerical framework introduced in this study was applied to the present equation, with a rigorous evaluation of its performance conducted across a wide spectrum of parameters γ and m. Data on the experimental convergence order and computational accuracy, compiled in Tables 5 and 6, provide strong evidence for the scheme's efficacy. Also, a comparative examination of the absolute errors, as delineated in Tables 7 and 8, substantiates the precision of our methodology in contrast to the conventional techniques documented in [11, 26–28] for the parameters $\gamma = 2$ and $\tau = 0.1$. Graphical outputs depicting exact versus approximated solutions for

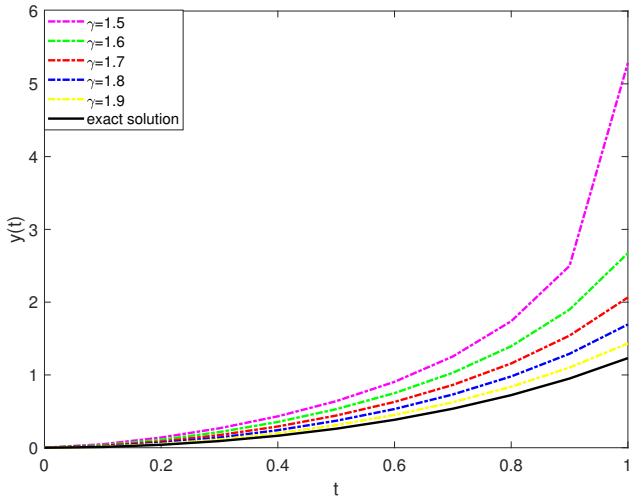

Figure 1: The exact and approximate solutions with several values γ in $\tau = 0.1$ for Example 5.1.

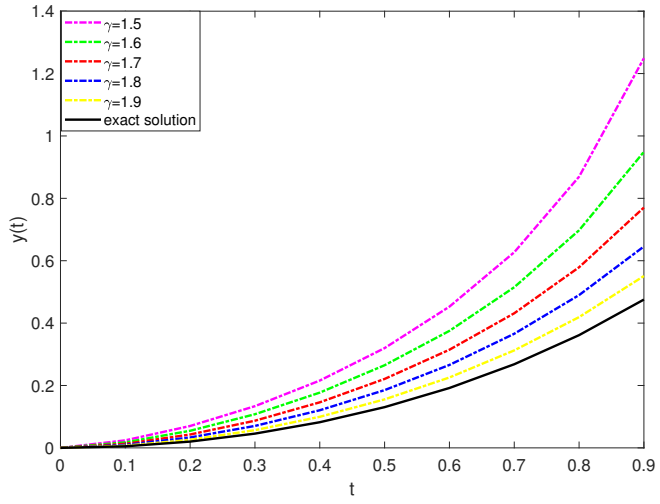

Figure 2: The exact and approximate solutions with several values γ in $\tau = 0.1$ for Example 5.2.

Table 2: The ℓ_∞ error of the yielded outcomes for some values of τ with $\gamma = 2$ in Example 5.1.

τ	ℓ_∞	co	CUP Time (s)
1/2	5.3354×10^{-02}	–	0.532
1/4	5.0924×10^{-03}	3.3891	0.531
1/6	1.2367×10^{-03}	3.4905	0.594
1/8	4.2922×10^{-04}	3.6784	0.719
1/10	1.8442×10^{-04}	3.7855	0.719
1/12	9.1419×10^{-05}	3.8492	0.687
1/14	5.0193×10^{-05}	3.8895	0.922
1/16	2.9753×10^{-05}	3.9162	1.422
1/18	1.8717×10^{-05}	3.9348	1.390
1/20	1.2347×10^{-05}	3.9482	16.485

Table 3: The ℓ_∞ error of the yielded outcomes for some values of τ with $\gamma = 2$ in Example 5.2.

τ	ℓ_∞	co	CUP Time (s)
1/2	2.6677×10^{-02}	–	0.656
1/4	2.5462×10^{-03}	3.3891	0.484
1/6	6.1835×10^{-04}	3.4905	1.375
1/8	2.1461×10^{-04}	3.6784	0.719
1/10	9.2213×10^{-05}	3.7855	1.766
1/12	4.5709×10^{-05}	3.8492	0.922
1/14	2.5096×10^{-05}	3.8895	1.844
1/16	1.4876×10^{-05}	3.9162	2.781
1/18	9.3588×10^{-06}	3.9348	4.125
1/20	6.1739×10^{-06}	3.9482	5.797

Table 4: The $\mathscr{E}_\infty$ error of the yielded outcomes with some values of m and γ in $T = 1$ for Example 5.2.

	$\gamma = 1.55$			$\gamma = 1.75$			$\gamma = 1.95$		
m	$T = 1$	$\mathscr{E}_\infty$	CPU	$T = 1$	$\mathscr{E}_\infty$	CPU	$T = 1$	$\mathscr{E}_\infty$	CPU
5	1.600604	–	2.812	0.930465	–	2.641	0.662684	–	2.672
7	1.601615	1.0111×10^{-03}	3.734	0.930817	3.5148×10^{-04}	3.547	0.662771	8.7403×10^{-05}	3.750
9	1.602554	9.3885×10^{-04}	4.813	0.930910	9.2688×10^{-05}	4.766	0.662792	2.0571×10^{-05}	4.906
11	1.603103	5.4919×10^{-04}	6.578	0.930941	3.1694×10^{-05}	6.234	0.662799	6.6681×10^{-06}	6.594
13	1.603417	3.1427×10^{-04}	8.266	0.930954	1.2857×10^{-05}	8.047	0.662801	2.6464×10^{-06}	8.906
15	1.603603	1.8518×10^{-04}	10.797	0.930960	5.8830×10^{-05}	10.468	0.662802	1.2078×10^{-06}	10.516

$m = 5$ (Figures 2 and 3) across various γ values further verify the method's reliability and exhibit a clear convergence trend to the exact solution as γ approaches 2. The collective evidence from the numerical data in Table 5, 8, and the visualizations in Figures 3 and 4 firmly establishes the proposed algorithm as a precise

and effective solver for this category of nonlinear fractional problems.

Table 5: The ℓ_∞ error of the yielded outcomes for some values of τ with $\gamma = 2$ and $\xi_0 = 1$ in Example 5.3.

τ	ℓ_∞	co	CUP Time (s)
1/4	1.5763×10^{-04}	–	0.718
1/6	4.3816×10^{-05}	3.1575	0.828
1/8	1.5826×10^{-05}	3.5396	0.750
1/10	6.9465×10^{-06}	3.6903	0.703
1/12	3.4940×10^{-06}	3.7691	16.000
1/14	1.9399×10^{-06}	3.8169	18.812
1/16	1.1603×10^{-06}	3.8488	43.125

Table 6: The ℓ_∞ error of the yielded outcomes for some values of τ with $\gamma = 2$ and $\xi_0 = 2$ in Example 5.3.

τ	ℓ_∞	co	CUP Time (s)
1/4	1.6716×10^{-03}	–	0.546
1/6	4.1556×10^{-04}	3.4329	1.125
1/8	1.3973×10^{-04}	3.7884	0.703
1/10	5.8453×10^{-05}	3.9056	0.640
1/12	2.8413×10^{-05}	3.9566	12.828
1/14	1.5378×10^{-05}	3.9823	16.235
1/16	9.0189×10^{-06}	3.9964	73.937

6. Conclusion

This paper introduces a high-accuracy numerical technique for the fractional Bratu equation, founded on a unique block-structured algorithm incorporating quadratic Lagrange interpolation. The proposed method demonstrates fourth-order convergence $\mathcal{O}(\tau^4)$, with both theoretical analysis and numerical experiments confirming this optimal convergence rate. These tests also demonstrate the algorithm's confirm the accuracy against the other methods.

Conflicts of Interest. The authors declare that they have no conflicts of interest regarding the publication of this article.

Acknowledgments. We would like to thank editor and reviewers for taking the necessary time and effort to review the paper. We sincerely appreciate all your valuable comments and suggestions, which helped us in improving the quality of the paper.

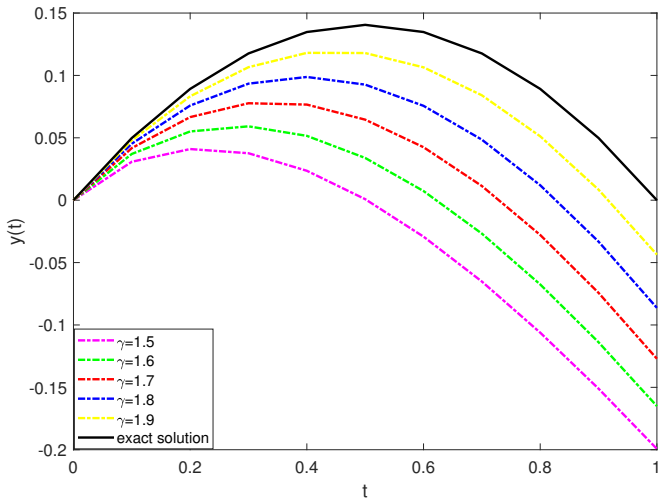

Figure 3: The exact and approximate solutions with several values γ in $\tau = 0.1$ for Example 5.3.

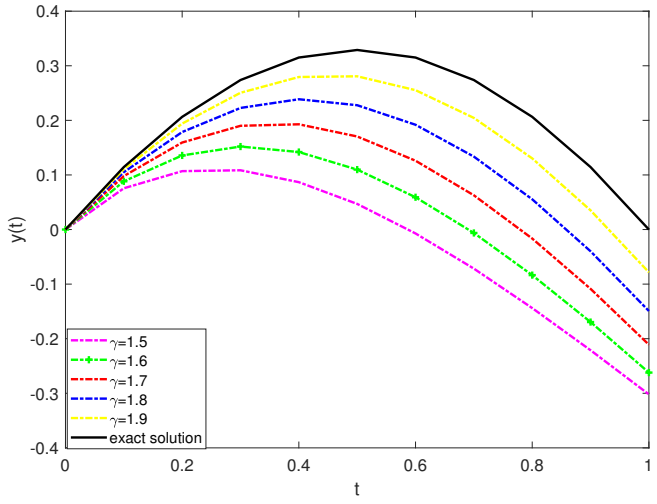

Figure 4: The exact and approximate solutions with several values γ in $\tau = 0.1$ for Example 5.3.

Table 7: Comparison of the ℓ_∞ with $\tau = 0.1$ and $\xi_0 = 1$ in Example 5.3.

t	[26]	[27]	[28]	[11]	Presented method
0.1	2.98×10^{-06}	1.98×10^{-06}	2.68×10^{-03}	5.27×10^{-05}	4.22×10^{-07}
0.2	5.46×10^{-06}	3.94×10^{-06}	2.02×10^{-03}	9.67×10^{-05}	8.50×10^{-07}
0.3	7.33×10^{-06}	5.85×10^{-06}	1.52×10^{-04}	1.30×10^{-04}	2.72×10^{-06}
0.4	8.50×10^{-06}	7.07×10^{-06}	2.20×10^{-03}	1.50×10^{-04}	1.39×10^{-06}
0.5	8.89×10^{-06}	9.47×10^{-06}	3.01×10^{-03}	1.57×10^{-04}	4.62×10^{-06}
0.6	8.50×10^{-06}	1.11×10^{-05}	2.20×10^{-03}	1.50×10^{-04}	1.42×10^{-06}
0.7	7.33×10^{-06}	1.26×10^{-05}	1.52×10^{-04}	1.30×10^{-04}	6.01×10^{-06}
0.8	5.46×10^{-06}	1.35×10^{-05}	2.02×10^{-03}	9.67×10^{-05}	8.88×10^{-07}
0.9	2.98×10^{-06}	1.20×10^{-05}	2.68×10^{-03}	5.27×10^{-05}	6.94×10^{-06}

Table 8: Comparison of the ℓ_∞ with $\tau = 0.1$ and $\xi_0 = 2$ in Example 5.3.

t	[26]	[27]	[28]	Presented method
0.1	1.72×10^{-05}	2.13×10^{-03}	1.52×10^{-02}	3.98×10^{-06}
0.2	3.26×10^{-05}	4.21×10^{-03}	1.47×10^{-02}	7.82×10^{-06}
0.3	4.49×10^{-05}	6.19×10^{-03}	5.89×10^{-03}	2.67×10^{-05}
0.4	5.28×10^{-05}	8.00×10^{-03}	3.25×10^{-03}	1.31×10^{-05}
0.5	5.56×10^{-05}	9.60×10^{-03}	6.98×10^{-03}	4.45×10^{-05}
0.6	5.28×10^{-05}	1.09×10^{-03}	3.25×10^{-03}	1.04×10^{-05}
0.7	4.49×10^{-05}	1.19×10^{-02}	5.89×10^{-03}	5.42×10^{-05}
0.8	3.26×10^{-05}	1.24×10^{-02}	1.47×10^{-02}	1.12×10^{-06}
0.9	1.72×10^{-05}	1.09×10^{-02}	1.52×10^{-02}	5.84×10^{-05}

References

[1] J. E. N. Valdés, The non-integer local order calculus, *Phys. Astron. Int. J.* **7** (2023) 163 – 168.

[2] M. Zheng, F. Liu and V. Anh, An effective algorithm for computing fractional derivatives and application to fractional differential equations, *Int. J. Numer. Anal. Model.* **18** (2021) 458 – 480.

[3] J. Xie and Y. Lakys, Application of nonlinear fractional differential equations in computer artificial intelligence algorithms, *Appl. Math. Nonlinear Sci.* **8** (1) (2023) 1145 – 1154.

[4] K. Hattaf, On the stability and numerical scheme of fractional differential equations with application to biology, *Computation* **10** (2022) #97, https://doi.org/10.3390/computation10060097.

[5] J. L. Suzuki, M. Gulian, M. Zayernouri and M. D'Elia, Fractional modeling in action: a survey of nonlocal models for subsurface transport, turbulent flows,

and anomalous materials, *J. Peridyn. Nonlocal. Model* **5** (2023) 392 − 459, https://doi.org/10.1007/s42102-022-00085-2.

[6] C. D. Constantinescu, J. M. Ramirez and W. R. Zhu, An application of fractional differential equations to risk theory, *Finance Stoch.* **23** (2019) 1001 − 1024, https://doi.org/10.1007/s00780-019-00400-8.

[7] Y. Q. Wan, Q. Guo and N. Pan, Thermo-electro-hydrodynamic model for electrospinning process, *Int. J. Nonlinear Sci. Numer. Simul.* **5** (2004) 5 − 8.

[8] A. A. Kilbas, H. M. Srivastava and J. J. Trujillo, *Theory and applications of fractional differential equations*, Elsevier, 2006.

[9] S. Kumar and V. Gupta, A polynomial-based operational matrix approach to solve fractional-order Bratu-type problems, *Nonlinear Complex Data Sci.* **25** (2025) 437 − 456.

[10] J. He and C. Cao, A new neural network method for solving Bratu type equations with rational polynomials, *Int. J. Mach. Learn. & Cyber.* **16** (2025) 1355 − 1369, https://doi.org/10.1007/s13042-024-02340-y.

[11] S. Latif, M. Amin, S. Mushtaq and N. Iftikhar, Spline based numerical algorithm for solving Bratu-type equations, *Kashf Journal of Multidisciplinary Research*, **2** (2025) 51 − 63.

[12] P. Pirmohabbati, A. H. Refahi Sheikhani and A. Abdolahzadeh Ziabari, Numerical solution of nonlinear fractional Bratu equation with hybrid method, *Int. J. Appl. Comput. Math.* **6** (2020) #162.

[13] A. Khalouta, New technique to accelerate the convergence of the solutions of fractional order Bratu-type differential equations, *J. Sci. Arts* **23** (2023) 497 − 512.

[14] G. Alhamzi, A. Gouri, B. S. T. Alkahtani and R. S. Dubey, Analytical solution of generalized Bratu-type fractional differential equations using the homotopy perturbation transform method, *Axioms* **13** (2024) #133, https://doi.org/10.3390/axioms13020133.

[15] A. Khalouta and A. Kadem, Solution of the fractional Bratu-type equation via fractional residual power series method, *Tatra Mt. Math. Publ.* **76** (2020) 127 − 142.

[16] A. Khalouta and A. Kadem, A new reliable method and its convergence for nonlinear second-order fractional differential equations, *Tbilisi Math. J.* **13** (2020) 133 − 143, https://doi.org/10.32513/tbilisi/1601344903.

[17] M. Izadi and H. M. Srivastava, Generalized bessel quasilinearization technique applied to bratu and lane-emden-type equations of arbitrary order, *Fractal Fract.* **5** (2021) #179, https://doi.org/10.3390/fractalfract5040179.

[18] G. Swaminathan, G. Hariharan, V. Selvaganesan and S. Bharatwaja, A new spectral collocation method for solving Bratu-type equations using Genocchi polynomials, *J. Math. Chem.* **59** (2021) 1837 – 1850, https://doi.org/10.1007/s10910-021-01264-0.

[19] X. Zhang and J. Cao, A high order numerical method for solving Caputo nonlinear fractional ordinary differential equations, *AIMS Math.* **6** (2021) 13187 – 13209.

[20] R. K. Lodhi, S. F. Aldosary, K. S. Nisar and A. Alsaadi, Numerical solution of non-linear Bratu-type boundary value problems via quintic B-spline collocation method, *AIMS Math.* **7** (2022) 7257 – 7273, https://doi.org/10.3934/math.2022405.

[21] R. Gharechahi, M. Arab Ameri and M. Bisheh-Niasar, High order compact finite difference schemes for solving Bratu-type equations, *J. Appl. Comput. Mech.* **5** (2019) 91 – 102, https://doi.org/10.22055/jacm.2018.25696.1288.

[22] H. Singh, A. K. Singh, R. K. Pandey, D. Kumar and J. Singh, An efficient computational approach for fractional Bratu's equation arising in electrospinning process, *Math. Methods Appl. Sci.* **44** (2021) 10225 – 10238, https://doi.org/10.1002/mma.7401.

[23] E. Keshavarz, Y. Ordokhani and M. Razzaghi, The Taylor wavelets method for solving the initial and boundary value problems of Bratu-type equations, *Appl. Numer. Math.* **128** (2018) 205 – 216, https://doi.org/10.1016/j.apnum.2018.02.001.

[24] M. A. Z. Raja, R. Samar, E. S. Alaidarous and E. Shivanian, Bio-inspired computing platform for reliable solution of Bratu-type equations arising in the modeling of electrically conducting solids, *Appl. Math. Model.* **40** (2016) 5964 – 5977, https://doi.org/10.1016/j.apm.2016.01.034.

[25] C. Li and M. Cai, *Theory and Numerical Approximations of Fractional Integrals and Derivatives*, SIAM, 2019.

[26] H. Caglar, N. Caglar, M. Ozer, A. Valaristos and A. N. Anagnostopoulos, B-spline method for solving Bratu's problem, *Int. J. Comput. Math.* **87** (2010) 1885 – 1891, https://doi.org/10.1080/00207160802545882.

[27] S. A. Khuri, A new approach to Bratu's problem, *Appl. Math. Comput.* **147** (2004) 131 – 136, https://doi.org/10.1016/S0096-3003(02)00656-2.

[28] N. Romero, Solving the one dimensional Bratu problem with efficient fourth order iterative methods, *SeMA J.* **71** (2015) 1 – 14, https://doi.org/10.1007/s40324-015-0041-1.

Hadis Azin
Department of Mathematics,
Faculty of Mathematical Sciences,
Alzahra University,
Tehran, I. R. Iran
e-mail: h.azin@alzahra.ac.ir

Yadollah Ordokhani
Department of Mathematics,
Faculty of Mathematical Sciences,
Alzahra University,
Tehran, I. R. Iran
e-mail: ordokhani@alzahra.ac.ir